

UNCLASSIFIED

AD NUMBER
AD903279
NEW LIMITATION CHANGE
TO Approved for public release, distribution unlimited
FROM Distribution authorized to U.S. Gov't. agencies only; Test and Evaluation; 19 Sep 1972. Other requests shall be referred to Department of Defense Explosives Safety Board, Washington, DC.
AUTHORITY
DTIC Form 55

THIS PAGE IS UNCLASSIFIED

77

AD902279



GENERAL AMERICAN TRANSPORTATION CORPORATION



GENERAL AMERICAN RESEARCH DIVISION

7448 NORTH NATCHEZ AVENUE, NILES, ILLINOIS 60648 312/647-0000

Final Report

GARD Project No. 1540

EXPLOSION EFFECTS COMPUTATION AIDS

by

L. E. Fugelso
L. M. Weiner
T. H. Schiffman

Prepared For

Department of Defense Explosives Safety Board
Washington, D. C.


Under Contract DAHC-04-72-0012

by .

General American Research Division
General American Transportation Corporation
Niles, Illinois

June 1972

Distribution limited to U.S. Gov't. agencies only.
Test and Evaluation; 18 SEP 72 Other requests
for this document must be referred to



ABSTRACT

Computational aids for the rapid assessment of potential hazards from blast and fragments during the accidental detonation of stored munitions were prepared. Four munitions, the MK82 500-lb bomb, the M117 750-lb bomb, the M107 155-mm shell and the M437A2 175-mm shell, stored in module type open barricaded pads, in above ground magazines and in standard earth covered igloos were considered. Targets considered included personnel standing in the open, frame structures, and unarmored military vehicles.

For the blast damage, this information is presented on a circular slide rule; for fragment damage, the information is presented in graphical form.

FOREWORD

This final technical report, entitled "Explosion Effects Computation Aids" was prepared for the Department of Defense Explosives Safety Board by General American Research Division of General American Transportation Corporation, under Contract DAHC-04-72-0012. The period of performance of the contract was November 15, 1971 through June 30, 1972.

LTC. J. D. Coder, USA served as Technical Coordinator and Dr. T. A. Zaker as the Technical Monitor for this contract. Mr. R. D. Perkins, DDESB, provided technical comment and criticism. Acknowledgement is made to Mr. Carl E. Rathmann of the GARD staff for performing several of the calculations reported here.

TABLE OF CONTENTS

<u>Chapter</u>	<u>Page</u>
ABSTRACT	ii
FOREWORD	iii
1 INTRODUCTION	1
2 FACTORS	3
3 BLAST EFFECTS	6
3.1 Blast-Range Parameters from a Hemispherical Charge	6
3.2 Igloo Effects	10
4 DAMAGE CRITERIA	13
4.1 Damage to Frame Structures	13
4.2 Injury to Personnel	18
4.3 Damage to Trucks	21
5 SUMMARY OF EQUATIONS TO BE USED FOR PREPARATION OF THE SLIDE RULE	23
6 DESCRIPTION OF THE SLIDE RULE	26
7 FRAGMENT HAZARDS	32
8 INJURY AND DAMAGE CRITERIA	35
9 FRAGMENT DATA	38
9.1 Single-Munition Fragment Density	38
9.2 Stacked-Munition Fragment Density	43
9.3 Damage Probability	46
10 CRITIQUE OF FRAGMENT HAZARD EVALUATION	49
REFERENCES	51

LIST OF FIGURES

<u>Figure</u>		<u>Page</u>
1	Blsst Parameters for a Hemispherical Source	7
2	Blast Pressure Reduction from Earth Covered Igloos at $\lambda = 35$	11
3	Isodamage Curves for a Frame Structure Damaged by Air Blast	17
4	Front Side of Slide Rule	27
5	Back Side of Slide Rule	28
6	Vulnerability of Standing Personnel to Fragments	36
7	Single Munition Fragment Density vs Range Munition - MK82 500-lb Bomb	39
8	Single Munition Fragment Density vs Range Munition - M117 750-lb Bomb	40
9	Single Munition Fragment Density vs Range Munition - M107 155-mm Shell	41
10	Single Munition Fragment Density vs Range Munition - M437A2 175-mm Shell	42
11	Schematic Figure to Show Basis for Approximation of Far-Field Fragment Density from Stack Munition	45
12	Calculated Fragment Density for Stacked Munitions from the Single Munition Model	47

LIST OF TABLES

<u>Table</u>		<u>Page</u>
1	Weapon Characteristics	4
2	Equivalent Factors for Various Explosives Relative to TNT	3
3	Effective Yield for Selected Munitions	9
4	Damage Levels at 10^6 lbs TNT	13
5	Critical Overpressures for Lung Damage to Humans	19
6	Probability of Eardrum Rupture	19
7	Lethality Due to Critical Impact Velocity and Critical Impulse	20
8	Damage Levels for Selected Targets	24
9	Energy Levels Associated with Personnel Injury from Fragments	37
10	Ranges at Which Fragment Densities (Sector Averages) Are 1 Per 600 Sq. Ft. (After Feinstein 1972)	43

CHAPTER 1

INTRODUCTION

When a stack of munitions detonates accidentally, two major effects occur, (1) a strong blast wave is propagated and (2) a large number of fragments are propelled away from the stack. Compilation of available explosion effects information to estimate risk of damage or injury from blast and fragmentation at various distances from the source to the target led to the preparation of graphical and mechanical computation aids for rapidly assessing the potential hazards from these effects.

The targets are standing personnel in the open, frame structures and trucks. Four munitions were considered in the detailed evaluation: the 155-mm M107 projectiles, the 175-mm M437A2 projectiles, the MK82 500-lb bomb and the M117 750-lb bomb. These munitions are normally stored within earth-covered igloos, above ground magazines, or within earth revetments in amounts ranging from several units up to 500,000 lbs of explosive weight. Previous experimental studies on the accidental detonation of such stored munitions have established the minimum intermagazine separation distances to prevent communication of the explosions to adjacent magazines. The Department of Defense Explosives Safety Board has further established quantity-distance relationships for safety to various other targets, such as inhabited buildings and public highways. The need may arise for assessing the potential hazard to various targets which, for a variety of reasons, may not fall under the guidelines published by the DDESB. For example, a temporary munition storage area may be required in an area where houses already exist or where a number of personnel may normally be found during the course of the day. The computation aid, to be described in detail later,

allows the rapid assessment of the hazards to these potential targets and of the effects of deviations from the recommended quantity-distance.

Available data, both experimental and theoretical, were to be used in the preparation of the computation aids. Sufficient data on blast effects, both on the nature of the blast generated by the stack and on the response of the specified targets are available. This information was gathered and reduced into a form suitable for a mechanical aid. A circular slide rule was prepared to assess the blast damage. Less data were available for assessing fragment hazards, thus, the fragment hazard data is presented in graphical form.

First the description of the munitions and munition storage pertinent to the evaluation of these hazards are presented. Then a summary of the data available on blast effects is given, together with a description of the damage or injury levels associated with blast. The range-yield relations for such damage levels are given. Simplified, conservative relations suitable for representation on a mechanical computation aid are derived. The form of this data is suitable for representation on a circular slide rule, whose description is given.

Basic single munition for field fragment data is presented in graphical form. Approximate methods for estimating damaging fragment densities from stacks of munitions are presented.

CHAPTER 2

FACTORS

The several factors that describe the munition storage, the weapon characteristics, the stack characteristics and the mode of storage that are pertinent to the blast and shock and fragment phenomena are given below.

Four munitions were chosen for detailed study in this project. Other munitions and bulk explosives were given cursory treatment. The four munitions are the 155-mm and 175-mm shells and the 500-lb and 750-lb bombs. Table 1 presents the data on single rounds of these munitions. These four munitions are in extensive use, have a large range of the parameter charge weight to metal weight, C/M, and have four different explosive fillers.

Table 2 shows the equivalent TNT weight for each of the four explosives (JMEM 1970).

Table 2 EQUIVALENT FACTORS FOR VARIOUS
EXPLOSIVES RELATIVE TO TNT

Explosive	Factor
TNT	1.00
H-6	1.25
Tritonal	1.13
Comp. B	1.10

These munitions are normally stored in rectangular piles. The parameters describing the stack are the number of munitions in the two horizontal directions and the vertical direction, the total number of munitions in the stack, the spacing between individual munitions and the orientation of the munitions within the stack.

Table 1 WEAPON CHARACTERISTICS

Weapon	Designation	Explosive Filler	Total Weight, lb	Explosive Weight, lb	Length, Inches	Diameter, Inches	Charge Wt./Metal Wt. = C/M
500-lb Bomb	MK82	H-6	500	192	56.15	10.75	0.62
750-lb Bomb	M117	Tritonal	737	386	51.41	10.10	1.10
155-mm Shell	M107	TNT	94.8	15.1	26.80	6.10	0.19
175-mm Shell	M437A2	Comp. B	144	30.8	34.50	6.90	0.28

The normal storage of the munitions is within one of three barricaded structures. The munitions may be surrounded by an earthen revetment such that the line of sight from the top of the munition stack to the top of the earth mound is greater than 2° from the horizontal. This revetment is normally on three sides, only the fourth side is open for access to the stack. The munitions may be stored within an earth covered, steel arch igloo. The earth cover is at least two feet thick at the crown and covers the top sides and rear wall; the front wall is concrete with steel doors. Typical dimensions of such a structure are 26 feet wide and 60 to 80 feet long. The munitions also may be stored in above ground magazines, which are structures with concrete walls. Typical plan dimensions of a magazine are approximately equivalent to the igloo dimensions.

CHAPTER 3

BLAST EFFECTS

When the stack of munitions accidentally detonates, an intense heat wave is propagated into the area surrounding the stack. The stack is roughly cubical and the orientation of the stack is unknown. Blast effects are approximated by determining the blast from a hemisphere of the same effective yield. The effective yield is the total equivalent TNT yield reduced to account for the energy lost to the fragments. Because of the configuration of the stack, the blast propagation is enhanced in certain directions; the maximum enhancement is evaluated and selected. The effect of a barricade or magazine may reduce the blast effects at a distance. Each of these effects is discussed below.

3.1 Blast-Range Parameters from a Hemispherical Charge

The blast-range parameters from the detonation of a hemisphere of TNT are chosen as the starting point for the evaluation of blast from the stored munitions. These parameters have been established by Kingery (1966) from compilations of experimental data covering a wide range of explosive weight. The parameters are peak overpressure, positive phase impulse and positive phase duration of the pressure profile. These are plotted in Figure 1 as functions of the independent variable, $\lambda = R/W^{1/3}$ where R is the distance from the center of the hemisphere in feet, and W is the charge weight in pounds of TNT. Peak overpressure scales with the ambient absolute pressure, p, and impulse as the 2/3 power of p in atmospheres of equal temperature, provided the distance is scaled inversely as the 1/3 power of p. Also plotted is the dynamic overpressure impulse adapted from Richmond and Fletcher (1971) for a hemispherical TNT source.

When a munition, such as those considered here, detonates, not all of the energy released goes into the blast wave. A fraction of the explosive energy is used to break up the case and to propel the fragments. Several

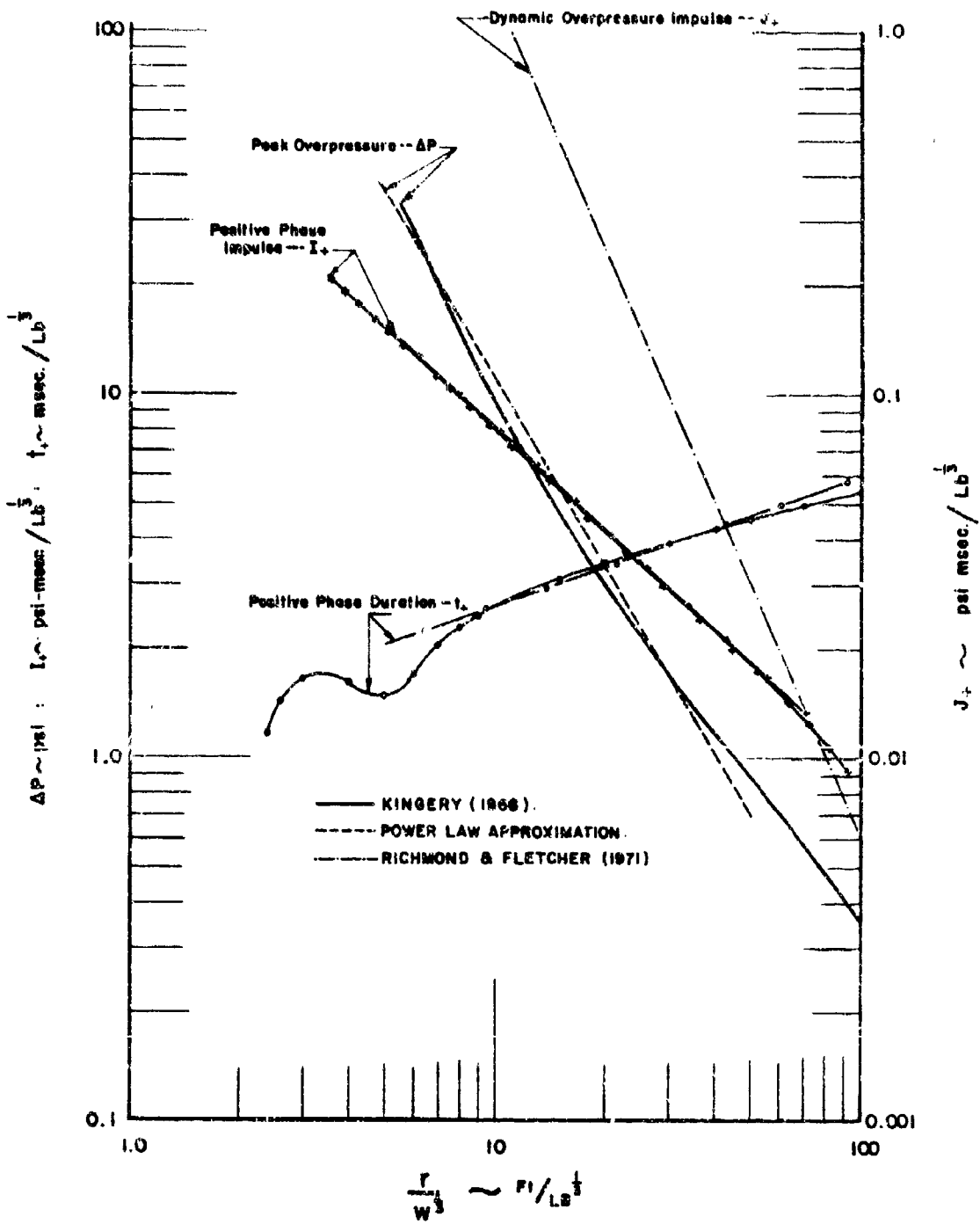


Figure 1 BLAST PARAMETERS FOR A HEMISPHERICAL SOURCE

estimates of the energy available to the blast wave based on theory and experiment are reported in the literature. The most common estimate of the energy available to the blast wave is the modified Fano formula (JME 4, 1970).

$$\frac{W_{\text{eff}}}{W} = 0.6 + 0.4 \left(1 + \frac{2}{C/M}\right)^{-1}$$

where: W_{eff} is the energy available for blast
 C/M is the charge weight-to-metal-weight ratio.

Table 3 shows this ratio for the four munitions considered. The charge weight in the ratio C/M is taken as the equivalent TNT weight.

The detonation of charge which has a shape other than spherical or hemispherical propagates a blast wave which shows a more complex spatial structure. Experiments have been conducted on the detonation of rectangular parallelepipeds (Adams, Sarmousakis and Sperraza, 1949); cylinders and disks of explosive material (Wisotski and Snyder, 1965; Fugelso, Fields and Byrne, 1971). For cubes and cylinders with $L/D = 1$, the peak overpressure versus range in the direction normal to a face or to the axis of the cylinder is enhanced relative to the same overpressure-range curve for hemispherical charge. In the overpressure range $1 \leq \Delta P \leq 40$ psi, the ratio between the two curves ranges between 1.1 and 1.5, with a mean value of 1.2. Once an increase in overpressure is established, this amplification persists at least to ranges where the overpressure is about 1.0 psi. An experiment on the detonation of a disk array of TNT shows the persistence of the amplification factor to overpressure of 0.1 psi (Fugelso, Fields and Byrne, 1971). In other directions, the peak overpressure range curves for the angles and cylinders can be less than hemispherical curves. In the extreme geometry of disk, the maximum amplification is about 1.5 in the same overpressure range.

Table 3 EFFECTIVE YIELD FOR SELECTED MUNITIONS

Munition	Explosive	Charge Wt., lb.	Equivalent Wt. TNT, lb.	Effective C/M	Fano Factor	Effective Wt. TNT, lb.
MK 82	H-6	192	240	0.78	0.712	171
M117	Tritonal	386	436	1.24	0.753	328
M107	TNT	15.1	15.1	0.19	0.635	9.58
M437A2	Comp. B	30.8	33.9	0.30	0.652	22.10

An earth revetment or barricade has a negligible effect on the propagation of blast at large distances from the barricade (Wiedermann, 1971). The blast is reduced at the ground for a short distance beyond the revetment ($r < 5 h$, where h is the height of the revetment), but the blast wave reforms at longer distances.

3.2 Igloo Effects

When the stack is contained within an earth-covered igloo, the blast wave at large range is reduced as a fraction of the blast energy is absorbed in breaking up the earth cover and in the energy of the fragments of the structure. A sequence of experiments (ANESB 1947, 1946a, 1946b) evaluated the attenuation of the blast as a function of the earth cover-weight-to-charge-weight ratio. Figure 2 shows the attenuation of the peak overpressure as a function of this ratio. The attenuation factor is the ratio of measured overpressures at a fixed scaled distance. The expected peak overpressure without the igloo is roughly 3 psi. For a given value of the cover-to-charge ratio, an effective charge weight can be defined by

$$\frac{\Delta P(\text{covered})}{\Delta P(\text{open})} = \left(\frac{W_{\text{eff}}}{W}\right)^{1/3} = k^{1/3}$$

The range of this factor is quite small for the range of typical igloo size and explosive contents. For the purposes of preparing a computation aid, a single value of k was chosen, rather than requiring the knowledge of the cover-to-charge ratio. The single value was chosen by considering a standard igloo 26 ft x 80 ft completely filled with munitions with a total charge weight of 200,000 pounds of TNT. For this configuration,

$$k \approx 0.8$$

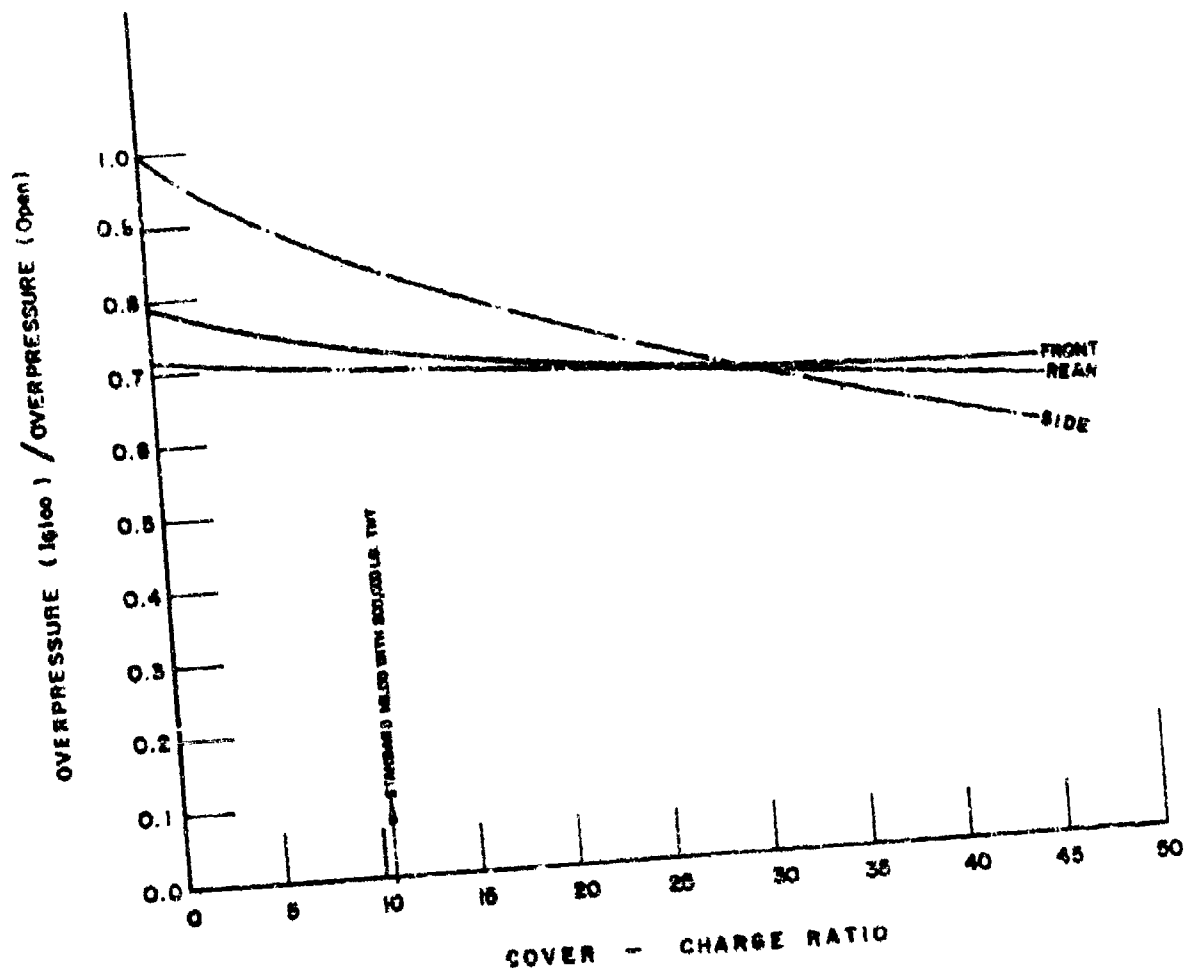


Figure 2 BLAST PRESSURE REDUCTION FROM EARTH COVERED IGLOOS
AT $\lambda = 38$

The blast parameter from the detonation of a stored munition then is represented by the blast from an equivalent hemisphere, where the equivalent yield is calculated by

$$W_{\text{stack}} = 1.2 W k F$$

where

W is the total charge weight of the stack in lb. of TNT,

F is the modified Fano formula using C/M,

k is an attenuation factor for the mode of storage

k = 1.0, munitions stored in the open or contained within an earth
revetment or in an above ground magazine

k = 0.8, munitions stored within a standard steel arch, earth-
covered igloo.

CHAPTER 4

DAMAGE CRITERIA

Three targets are selected for evaluation of potential damage from blast. They are standing personnel in the open, frame structures and trucks.

4.1 Damage to Frame Structures

Damage to frame structures is caused by failure of structural components in response to the overpressure as a function of time. Some tests of the damage of frame structures by blast from various yield explosions have been reported in the literature (Wilton, 1970) with assessments of the damage. Johnson (1967) generated an empirical formula for relating the range at which specified damage levels occur. If R_1 is the range at which a selected damage level occurs for explosive yield W_1 , then the range, R , at which the same damage occurs for yield, W is

$$\frac{R}{R_1} = \left(\frac{W}{W_1} \right)^{0.435}$$

The damage levels at 10^6 lb. TNT, are summarized in Table 4.

Table 4

DAMAGE LEVELS AT 10^6 lb TNT

Damage	ΔP , psi	Range (R), ft
Threshold Glass Breaking	0.25	12,700
10% Damage	0.9	4,500
50% Damage	3.0	1,990
90% Damage	5.0	1,440

This approach was severely criticized by Westine (1971), who suggested an alternate approach, essentially fitting the same damage level through a curve of the form:

$$R = \frac{kW^{1/3}}{(a + \frac{b}{W} + \frac{c}{W^2})^{1/6}}$$

where k, a, b and c are empirical constants.

This form is asymptotic to a peak overpressure criterion at large yield and to an impulse criterion at small yields.

The limiting forms suggested an alternate procedure for determining the isodamage curves in the R-W plane. A bilinear relation between peak overpressure and positive phase impulse was derived which provides an upper bound in the range.

The two bounding forms for a pressure-duration relationship that must be satisfied to just break a structural element are:

$$\begin{aligned} \Delta P &= \Delta P_c & t_x &> \frac{1}{2\omega} \\ \Delta P &= \frac{\Delta P_c}{2\omega t_x} & t_x &< \frac{1}{2\omega} \end{aligned}$$

For a single structural element ΔP_c is the overpressure at which the element fails under an infinite duration step load and ω is its natural frequency. The parameter t_x is defined:

$$\Delta P t_x = I_+$$

where I_+ is the positive phase impulse

In the range $0.8 \leq \Delta P \leq 40$ psi, the following approximation holds (taken by least square fits to the Kingery TNT hemisphere curves):

Peak overpressure:

$$\Delta P = 569.5 \lambda^{-1.711} \text{ psi}$$

where $\lambda = R/W^{1/3}$

More generally, we consider $\Delta P = f(\lambda)$, but we will use the power law expression here to illustrate the technique:

Positive phase impulse:

$$I_+ = 67.42 \lambda^{-0.9243} W^{1/3} \text{ psi-msec}$$

Positive phase duration:

$$t_+ = 1.188 \lambda^{0.3473} W^{1/3} \text{ msec}$$

where $W =$ yield in pounds TNT

$R =$ range in feet

In terms of the blast parameter:

$$t_x = 0.1184 W^{1/3} \lambda^{0.7879} \text{ msec}$$

The first form is the bound for a load whose duration is long compared to the period of free vibration of the structure. It is dependent on a peak value of overpressure. The second form is a bound for a load whose duration is short compared to the period of the structure and is an impulse criterion. We have taken the lower bound of overpressure in both cases so that we will obtain an upper bound for range in the yield-range plane. We can express both forms in the yield-range plane by expressing P and t_x in terms of W and R . We take the smaller range at fixed yield to establish the yield-range isodamage curve.

$$W = \left(\frac{P_c}{569.5} \right)^{1.753} R^3 \quad W > W_1 (R)$$

$$W = \left(\frac{P_c}{134.86} \right)^{1.560} R^{1.440} \quad W < W_1 (R)$$

where $W_1(R)$ is:

$$W_1(R) = (.2368 \omega)^{-14.14} R^{-11.14}$$

Since the average frame structure has several structural components with different values of ΔP_c for failure, we take definite values of ΔP_c as representative of the degree of major structural damage to frame structure. These are generated from Wilton's (1970) assessment of damage to frame houses by large yield blasts. Approximately 10% of his total damage is deducted, since the plaster and glass damage are included in this figure. For the threshold of structural damage, $\Delta P_c = 0.9$ psi; for 50% structural damage, $\Delta P_c = 3.0$ psi; and for 90% structural damage, $\Delta P_c = 5.0$ psi.

These curves are plotted in Figure 3. The example plotted in Figure 3 is for structures whose natural period is 160 msec/cycle, which is typical of a wood rafter. Also plotted are Wilton's experimental points and Custard's et. al. (1970) calculation of damage based on Sewell's condition that the impulse exceeds a critical value with a critical period. The tested structure is plotted with an indicated damage level including glass and plaster damage and major structural damage. Johnson's empirical fit for the 10% damage level is also included. The World War II data on A-, B-, and C-level damage from 500-4000 lb. bombs on small steel factories are also plotted (Kennedy, 1946). Westine (1971) reports a fit of the type presented earlier in this section for brick houses. For complete destruction, this is:

$$R = \frac{9.5 W^{1/3}}{[1 + (\frac{7000}{W})^2]^{1/6}}$$

This curve is also plotted. It agrees with the A-level damage (or complete destruction) data and also agrees with $\Delta P_c = 12$ psi for this type of structure (Wolosewick, private communication). Also included is the threshold for glass breakage which is taken as $\Delta P_c = 0.25$ psi.

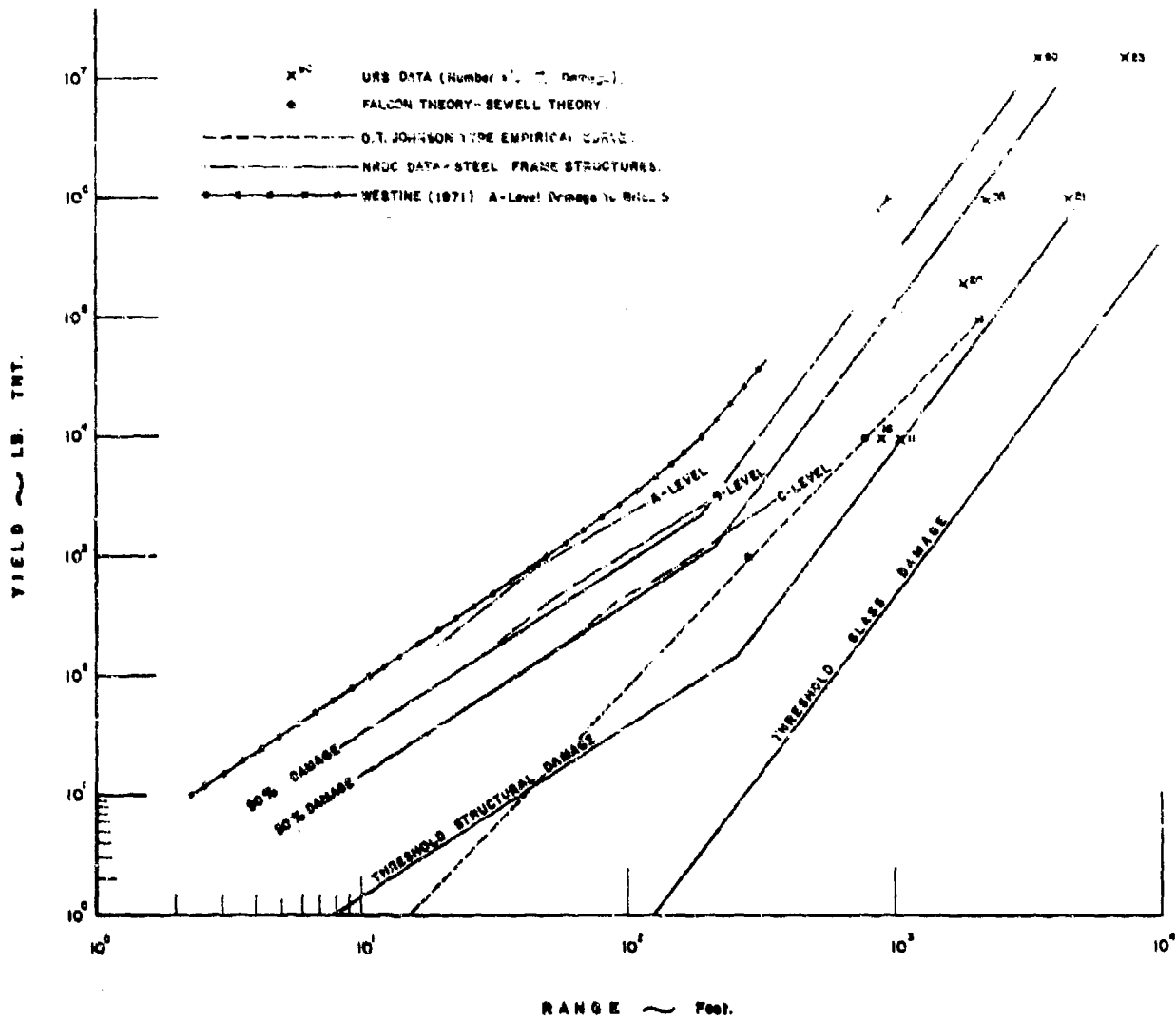


Figure 3 ISODAMAGE CURVES FOR A FRAME STRUCTURE DAMAGED BY AIRBLAST.

The value of W_1 for these damage levels occurs between 100 and 1000 lb. of TNT. A reasonable approximation for the damage is given by the overpressure criterion. The ranges at which damage is overestimated occur for very small charges. The hazard evaluation from munition storage normally involves larger total charge weights, and the overestimate of range (which is conservative) for small charges is not considered important.

4.2 Injury to Personnel

Personnel are affected by blast waves in two major modes: (1) by damage to internal organs by overpressure, denoted primary damage; and (2) by translation followed by striking an obstacle, denoted tertiary damage. The former damage mechanism to lungs has been investigated by Bowen et. al. (1968) and von Gierke (1968), and to ears by Hirsch (1966). The latter mechanism has been investigated by Richmond et al. (1966, 1968) and Bowen et.al. (1968).

Data on primary injury to personnel have been obtained by experimentally determining overpressure-duration relationships for animals, and extrapolating these to humans. The relationship to some specified degree of lung damage fatality is:

$$\Delta P = \Delta P_c (1 + 6.76 t_+^{-1.064})$$

Table 5 shows the free field overpressure, ΔP_c , associated within various levels of lethality at infinitely large durations (Bowen et.al. 1968).

Table 5

CRITICAL OVERPRESSURES FOR LUNG DAMAGE TO HUMANS

Damage	Peak Overpressure, psi
Threshold	14.5
10% Lethality	17.5
50% Lethality	20.5
90% Lethality	25.5
99% Lethality	29.0

Von Gierke (1968) considered the human lung as a one-degree of freedom system with damping. The derived relationship has the same form as the damage criteria for the frame structures and is also very close to the empirical curve. For the human lung the fundamental frequency, ω , is between 100 and 1000 cps.

Eardrums are damaged in response to overpressure alone as the characteristic period of the ear vibration is small compared to the duration of a blast profile from one pound of TNT. Hirsch (1966) has established the relationship between the overpressure and the probability of eardrum rupture (Table 6).

Table 6

PROBABILITY OF EARDRUM RUPTURE

Free-Field Peak Overpressure, psi	Probability of Eardrum Rupture
2.4	Threshold
2.8	10%
6.3	50%
12.2	90%

Injury to personnel by tertiary effects is related to the maximum translation velocity that the body can attain during the blast. It is assumed that the injury is caused when the body strikes an obstacle at maximum velocity. The probability of lethality for body impact has been determined as a function of the impact velocity. Lethality criteria have also been determined for impact of the head against an obstacle. Table 7 shows the impact velocity associated with several levels of lethality (Richmond et.al. 1966).

TABLE 7
LETHALITY DUE TO CRITICAL IMPACT VELOCITY AND CRITICAL IMPULSE
(V_m in ft/sec and J_c in psi-msec)

Lethality	Body		Head	
	V_m	J_c	V_m	J_c
Threshold	20	83.6	13	54.3
50%	26	108.6	18	75.2
99%	30	125.4	23	96.1

The acceleration of the body in response to the blast is given by the dynamic overpressure impulse. The maximum translational velocity is related to this impulse by

$$V_m = C_D A J_+ / M$$

where: J_+ is the dynamic overpressure impulse

M is the mass of the body

C_D is the drag coefficient of the target, assumed here to be unity

A is the presented cross-section area of the body to the blast.

An approximation for the dynamic overpressure impulse for a hemispherical TNT source, adapted from the reflected spherical source of Richmond and Fletcher (1971) is

$$J_+ = 266.4 \lambda^{-2.3201} W^{1/3} \text{ psi-msec}$$

Each maximum translation velocity defines a critical level of the dynamic overpressure impulse, J_c . When $J_+ \geq J_c$, the damage is assumed to occur and the equality defines a yield-range curve for that level of lethality. We calculate J_c for a typical grown male adult, using a weight of 155 pounds and an area of 8 square feet. See Table 7.

4.3 Damage to Trucks

One source of blast damage to trucks results from overturning the vehicle. If the blast overpressure and dynamic pressure time histories are known, the turning of the vehicle can be calculated (Custard et.al. 1970). A second source of damage is the severe deformation of structural components in response to the overpressure.

For a vehicle subjected to broadside blast impulse, responding in rigid rotation about an axis at the ground surface in the plane of the front and rear wheels away from the explosion source, overturning occurs when the dynamic overpressure impulse, J_+ , exceeds the critical value, J_c , given by

$$J_c = (2mgd_o I_A)^{1/2} / C_D A h_c$$

where C_D is a drag coefficient, g is gravitational acceleration, and

$$d_o = (h_g^2 + b^2/4)^{1/2} - h_g$$

If the mass of the vehicle is uniformly distributed over the superstructure height, h , and width, b ,

$$I_A = m((b^2 + h^2)/12 + (d_o + h_g)^2)$$

where: I_A is the moment of inertia about the line through one front and rear wheel

$$I_A = m \left(\frac{b^2 + h^2}{12} \right) + d_o + h_c$$

m = mass of the truck

b = width of the truck

h = height of the truck

$$d_o = \frac{b^2}{2} + h_g^2 - h_g$$

h_g = height of center of gravity of the truck

h_c = height of center of the blast pressure

A = side area of truck presented to the blast wave.

The values of J_c for typical trucks range between 70 and 110 psi-msec for incipient overturning (Custard et.al. 1970). Ethridge (1961) measured the overturning and blast damage to jeeps and trucks side-on and face-on to the air blast from a 100-ton TNT hemispherical burst. Incipient overturning occurred for $110 \leq J_c < 170$ psi-msec. We take 90 psi-sec as a typical threshold value. When the truck is just barely overturned, it is not likely to be damaged severely and when it is righted, it can probably be driven away. When the dynamic overpressure impulse exceeds the threshold, the truck will be translated after overturning with increasing possibility of damage as the translation velocity increases. Tests of damage to parked trucks in response to blast from nuclear burst shows that the threshold of overturning is between 60 and 100 psi-msec and complete damage after overturning occurs when J_c is greater than 500 psi-msec (Glasstone, 1964). Ethridge's (1961) measurements of damage to blast overturned jeeps shows the severe damage limit between 250 and 350 psi-msec. We use a value of 300 psi-msec as the criterion for complete destruction to a military vehicle due to overturning.

Ethridge also measured damage to jeeps and trucks face-on to the explosion and found that no overturning occurred. Vehicles were damaged by severe distortion of structural components, such as hoods, frames, etc. This damage in relation to air blast is estimated in much the same manner as damage to frame structures. The criteria for levels of damage in this mode is overpressure. From Ethridge's experimental data, values of 6 psi for the threshold of damage and 30 psi as the level above which total damage occurs is selected.

CHAPTER 5

SUMMARY OF EQUATIONS TO BE USED FOR PREPARATION OF THE SLIDE RULE

The equation for yield-range to be used for preparation of a mechanical computation aid are summarized in this chapter.

The effective yield in pounds of TNT that is available to the air blast is

$$W_{\text{Eff}} = 1.2W k F$$

where W is the total filler weight of explosive in the munition expressed in lb. of TNT. The total filler weight, W , is given by

$$W = n W_1 f$$

where n is the number of munitions in the stack, W_1 is the filler weight in one munition and f is the explosive equivalence factor to convert pounds of filler explosive to pounds of TNT. F is the modified Fano formula to account for the fraction of explosive energy available for blast

$$F = 0.6 + \frac{0.4}{1 + \frac{2}{C/M}}$$

where

$$C = W_1 f$$

and M is the metal or case weight of the munition.

For thin-cased munitions or bulk explosives, $F = 1$

The factor k is defined

$k = 1.0$, munitions stored above ground, within earth
revetments or in above ground magazines

$k = 0.8$, munitions stored in standard steel and
earth covered igloos.

The range-yield curves for damage to the selected targets are based on the fact that the damage levels can be related to either (1) values of the

peak overpressure or (2) the dynamic overpressure impulse. The peak overpressure is given by a function of the form

$$\Delta P = g\left(\frac{R}{W_{\text{Eff}}^{1/3}}\right) \text{ psi}$$

where $g(\lambda)$ is given by Kingery (1966).

The dynamic overpressure impulse is approximated by

$$J_+ = 266.4 \left(\frac{R}{W_{\text{Eff}}^{1/3}}\right)^{-2.3201} W_{\text{Eff}}^{1/3} \text{ psi}$$

The positive phase impulse (although not used for estimation of damages to these particular targets) is

$$I_+ = 67.424 \left(\frac{R}{W_{\text{Eff}}^{1/3}}\right)^{-0.92337} W_{\text{Eff}}^{1/3} \text{ psi}$$

When the values of either ΔP or J_+ are known for a given damage level, an algebraic expression for W_{Eff} as a function of R is obtained.

The damage levels associated with each target are summarized in Table 8.

Table 8

DAMAGE LEVELS FOR SELECTED TARGETS

Target	Damage Level	Peak Overpressure, psi	Dynamic Overpressure Impulse, psi-msec
Frame Structure	Threshold Glass Breakage	0.25	
	Threshold Structure Damage	0.90	
	50% Structural Damage	3.00	
	Total Damage	5.00	

Table 8 (Continued)

Target	Damage Level	Peak Overpressure, psi	Dynamic Overpressure Impulse, psi-msec
Standing Personnel	Eardrum Rupture		
	Threshold	2.40	
	10% Rupture	2.80	
	50% Rupture	6.30	
	90% Rupture	12.00	
	Lung Hemorrhage		
	Threshold	14.50	
	10% Lethality	17.50	
	50% Lethality	20.50	
	90% Lethality	25.50	
	99% Lethality	29.50	
	Tertiary Damage		
	Body Impact		
	Threshold		84
	50% Lethality		109
90% Lethality		125	
Head Impact			
Threshold		54	
50% Lethality		75	
99% Lethality		96	
Truck	Threshold Overturning		90
	Total Damage Overturning		300
	Threshold Crushing	6	
	Total Crushing	30	

CHAPTER 6

DESCRIPTION OF THE SLIDE RULE

As a part of this program, a circular slide rule type computer was designed which presents to the user the information described above in a convenient and compact form. The computer utilizes both sides of a 10-inch disc and one slightly smaller movable disc on each side.

The front side of the computer deals with problems related to damage resulting from blast effects of explosives stored in bombs or shells. It is illustrated in Figure 4. The back of the computer deals with problems related to blast effects resulting from detonation of bulk explosives and explosives loaded in light-cased munitions where the casing factor is negligible. The back is illustrated in Figure 5.

The parameter which determines the effects of an explosion of a stack of weapons or a given amount of bulk explosives is the effective yield of the explosion in terms of pounds of TNT. This is determined on the slide rule by making one setting.

In the case of a stack of bombs or shells, one enters on the front of the computer by setting the number of weapons on the proper scale in the window at the top (labelled A in Figure 4) or by setting the weight of the explosive filler at the proper hairline at the top left of the computer (labelled B in Figure 4). This setting determines the effective yield, which is given in the window denoted by C, and determines all other pertinent damage effects, so that once this setting is made the top disc should not be moved.

The effective yield shown in this window takes into account the casing factor, the TNT equivalent of the particular explosive being considered, and

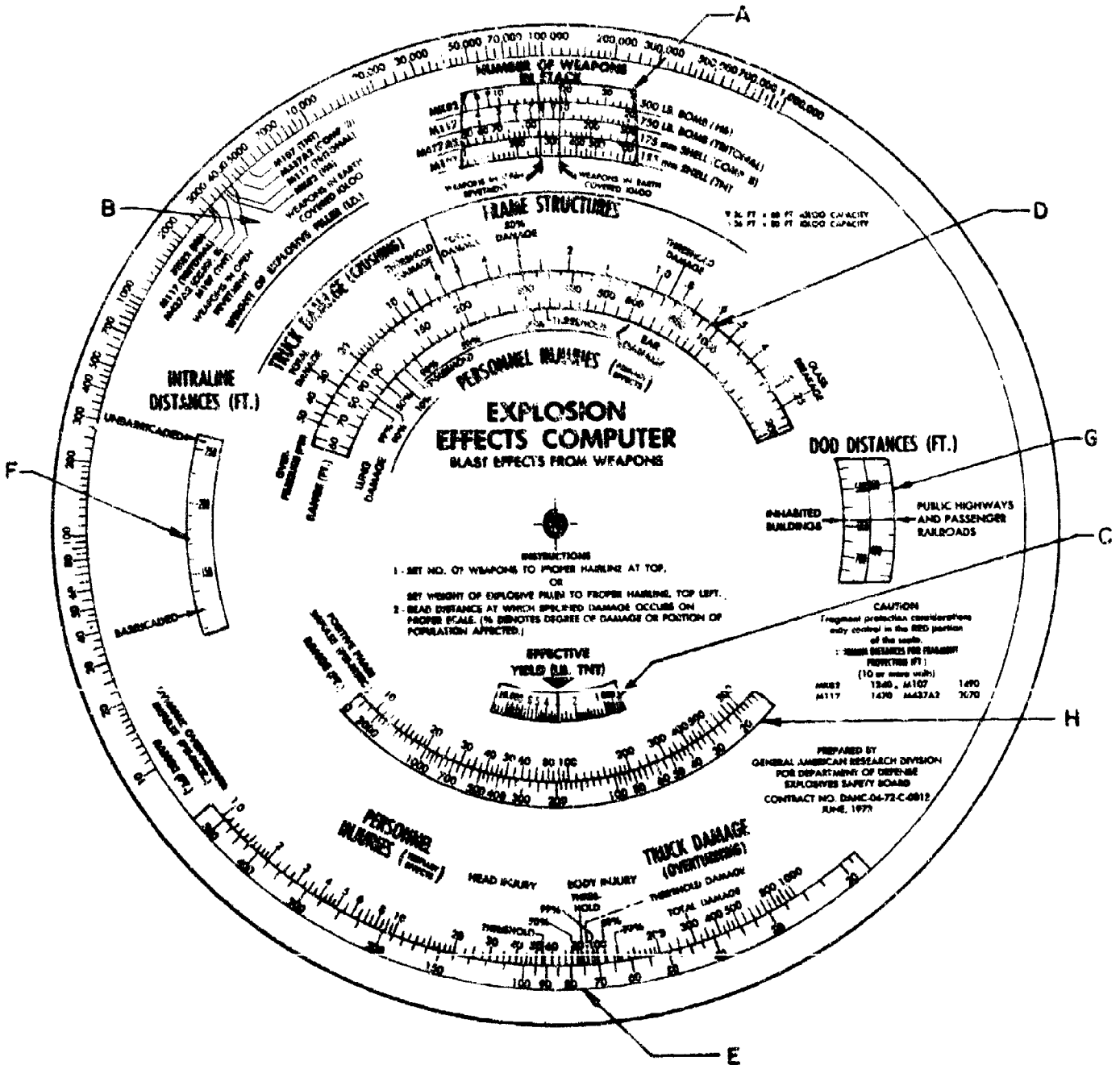


FIGURE 4. FRONT SIDE OF SLIDE RULE

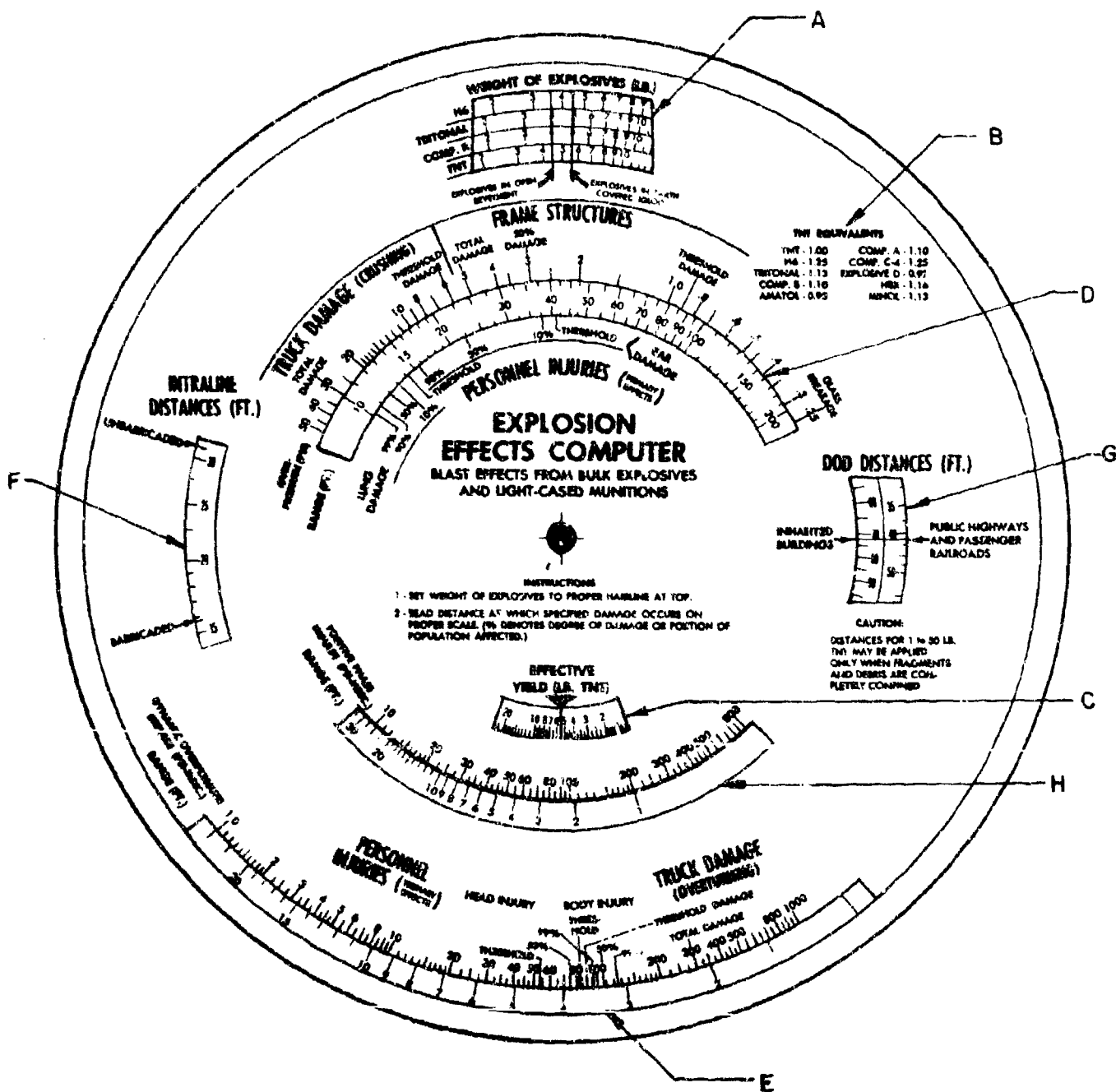
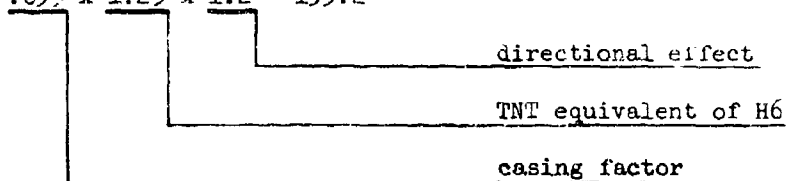


FIGURE 3, BACK SIDE OF SLIDE RULE

a factor of 1.2 to correct for the maximum directional effect since the blast wave is not uniform in all directions. For example, one MK82 bomb contains 192 pounds of H6. Thus, setting the black hairline to 1 on the MK82 scale yields:

$$192 \times .695 \times 1.25 \times 1.2 = 199.2$$



on the effective scale. In the case of weapons stored in earth covered igloos (where the red hairline is used), a factor of 0.8 is also included to account for the attenuation of the blast effects. Thus setting the red hairline to 1 on the MK82 scale yields $199.2 \times 0.8 = 159.36$ on the effective yield scale. These factors are based on information presently available from blast measurements and igloo tests. All effects scales described below are coordinated with the effective TNT yield in window C.

The scales denoted by D in Figure 4 give the relationship between the distance from the explosion and the peak overpressure occurring at that distance and are based on Kingery (1966). This scale indicates the distances at which glass breakage, threshold damage, 50 percent damage and total damage will occur to frame structures and threshold and total truck crushing damage due to a particular explosion. This scale also indicates the distances for threshold, 10, 50, and 90 percent of personnel incurring ear damage, and the distances for threshold, 10, 50, 90, and 99 percent of personnel incurring lung damage. These percentages refer to the degree of damage or to the portion of the population affected.

The scales denoted by E give the relationship between the distance from the explosion and the dynamic overpressure impulse occurring at that distance. The distances at which threshold, 50 and 99 percent of the population will incur head and body injuries and the distances at which threshold truck

overturning and total truck damage will occur is also given on these scales.

The scale denoted by F in Figure 4 gives the intraline distances for barricaded and unbarricaded weapons and is based on Table 5-6.3 in DOD publication 4145.27M, DOD Ammunition and Explosives Safety Standards, dated April, 1971. This table is based on the formulas $D = 9W^{1/3}$ for barricaded weapons and $D = 18W^{1/3}$ for unbarricaded weapons, where D = distance in feet. This scale, as well as the scales for DOD Distances (labelled G in Figure 4) are intended as guides for the user to indicate approximate distances, but the DOD manual referenced above should be consulted for compliance purposes.

The scales denoted by G in Figure 4, give the distances from the stack of weapons to inhabited buildings, highways and passenger railroads, and are based on Table 5-6.4 in DOD publication 4145.27M referenced above. If the reading should fall in the red portion of the scale, fragment protection considerations may override blast protection considerations. To determine whether this is the case, consult the table of minimum distances for the particular weapon being considered (directly below the window denoted G) if this minimum distance is greater than that indicated by the arrow, fragment protection considerations will control.

The scales indicated by H in Figure 4 gives the relationship between the distance from the explosion and the positive phase impulse at that distance.

The back of the computer deals with problems related to detonation of bulk explosives or explosives in thin-cased munitions. It is essentially the same as the front except that one enters by setting the hairline to the weight of the explosives on the proper scale in the window at the top, indicated by A in Figure 5. Once this setting is made, all the information is read exactly as described for the front of the computer except that for

DOD distances (read in window G), those distances for 1 to 50 lbs. TNT may be applied only when fragments and debris are completely confined. On this side of the computer, the effective yield contains all adjustment factors described on page 29 with the exception of the case factor.

For explosives other than the four indicated, the table of TNT equivalents (denoted by B in Figure 5) may be used to obtain a factor by which the weight of explosive should be multiplied to enter the TNT scale in window A (Figure 5). The damage effects may then be read as before.

It is also possible to solve inverse type problems on the computer. For example, it can be used to determine the maximum number of weapons of a certain type which may be stored in a stack a given distance from a building. This distance is set on the scale denoted G in Figure 4, and the number of weapons is read on scale A. Here again, one must determine whether blast effects or fragments will be the controlling factor.

CHAPTER 7

FRAGMENT HAZARDS

One objective of the contract is to determine the fragment hazards at large ranges due to accidental detonation of four selected munitions. The fragment patterns from single munitions and stacks of these munitions are considered; the munitions may be stored in the open, barricaded by earth revetments and contained within standard earth-covered igloos.

To assess fragment hazards, it would be desirable to have either theoretical predictions or experimental data which give fragment densities at fixed ranges as a function of the several parameters in the problem. We do not have this situation, either from theory or experiment. Experimental correlation between various configurations, e.g., single munition and stacked munitions of the same type, is not available, and theoretical correlations are as yet, poor. Predictions for single unbarricaded munitions and several isolated experimental values for barricaded and unbarricaded stacks are available.

A limited number of field tests of the detonation of stacked munitions have been carried out in the past. Two of these, the Arco, Idaho (ANESB, 1947, 1946a, 1946b) experiments and Eskimo I conducted by the Naval Weapons Center (Coder, 1971) had large numbers of munitions within earth-covered igloos. In the former case, fragment data were gathered in the first four shots. Experiments with large stacks not contained in igloos were conducted at Yuma (Kingery, 1971), and during the Big Papa experiments (Peterson, et al., 1968). In the former, an unusual stack geometry of 1 x 10 x 100 155-mm shells was unbarricaded. In the latter, mixed stack of 750-lb and 2,000-lb bombs was barricaded by an earth revetment. Unbarricaded 2 x 3 and

5 x 3 stacks of 750-lb bombs were detonated in an experiment conducted at Naval Weapons Center (Feinstein and Nagaoka, 1971). Model studies of fragmentation in stacks using paper cylinders coated with buckshot have been conducted by IITRI to obtain data on the fragment interaction process (Feinstein, 1970 and Nagaoka, 1971).

There seems to be no experimental data on far-field fragment distributions from single munitions. Close-in data for the munitions, yielding fragment distributions and initial fragment velocities as functions of the angular coordinates centered in the munitions are available; the best current source is the JMEM manuals, (JMEM 1970). A large number of reports deal with calculation of fragments near the munitions.

A limited number of theoretical calculations of far-field fragment distributions from a single munition have been made (Feinstein, 1972; Zaker et al., 1970). Without experimental verification of the far-field fragment distributions use of any theoretical calculation is on shaky ground.

Calculation of the far-field fragment distribution from unbarricaded stacks is a more complex problem because the fragments collide, fracture and interact, thus altering their initial velocity and distribution. Applying a simple multiplier, such as the number of munitions on the outer surface layer of the stack, to single-munition data is probably inadequate, although several such factors have been suggested. No calculations have been made of fragments in the far-field from either single munitions or stacked munitions within igloos.

The assessment of injury and damage criteria once the fragment density and terminal velocities are determined is better known. Damage levels can be related with some degree of reliability to the product of the fragment mass and its terminal velocity. The probability of damage can be computed

from the number density of fragments exceeding the damage criteria, and the presented area of the target. The probability of damage from many fragments can be calculated from the probability of damage from a single fragment.

To summarize, we have (1) theoretical calculations for far-field fragment densities from single, unbarricaded munitions, and (2) several measured far-field fragment densities from stacked munitions in a variety of configurations. Methods of extending the calculations to the stacked and/or barricaded configurations lack verification. Parametric representation of fragment densities from stacked and/or barricaded configurations is virtually nonexistent. Graphical and tabular presentations of the fragment densities calculations for a single munition are prepared. The approximations for passing from a single munition to stacks are discussed and presented. Damage levels are related to kinetic energy impact; these data are presented in tabular form also.

CHAPTER 8

INJURY AND DAMAGE CRITERIA

Data on the interaction of fragments and blast with the targets have been collected to determine damage criteria. The primary emphasis for fragment damage is on the personnel targets. Fragments injure personnel by perforating them or, if large enough, by crushing them. Feinstein (1971) gave a detailed summary of the fragment mass-striking velocity relationship for many mechanisms of injury. From these, a composite M-V curve using the 50-percent fatality criteria was proposed (Zaker et al., 1970). This is shown in Figure 6. Criteria for perforating the body are based on kinetic energy of the projectile at impact, i.e., a damaging fragment is one that satisfies:

$$\frac{MV_f^2}{2} \geq k$$

where: M is the mass of the fragment

V_f is the terminal velocity

k is the constant related to some specified damage level.

Feinstein (1971) summarized values of k for several types of perforation injuries. This mode is dominant for fragments with mass between 40 grams and 2 lb. Table 9 lists values of k for selected injury levels. The values are weighted averages of fragment-caused injury to vulnerable areas of the body, i.e., the thorax, head, abdomen and limbs. In a similar manner the crushing mode is represented by a momentum criterion:

$$MV_f \geq k_1$$

Fragment damage to frame structures and vehicles is by perforation of critical components. This mode of damage to frame structures is generally insignificant, as patching of the small holes that result are generally just

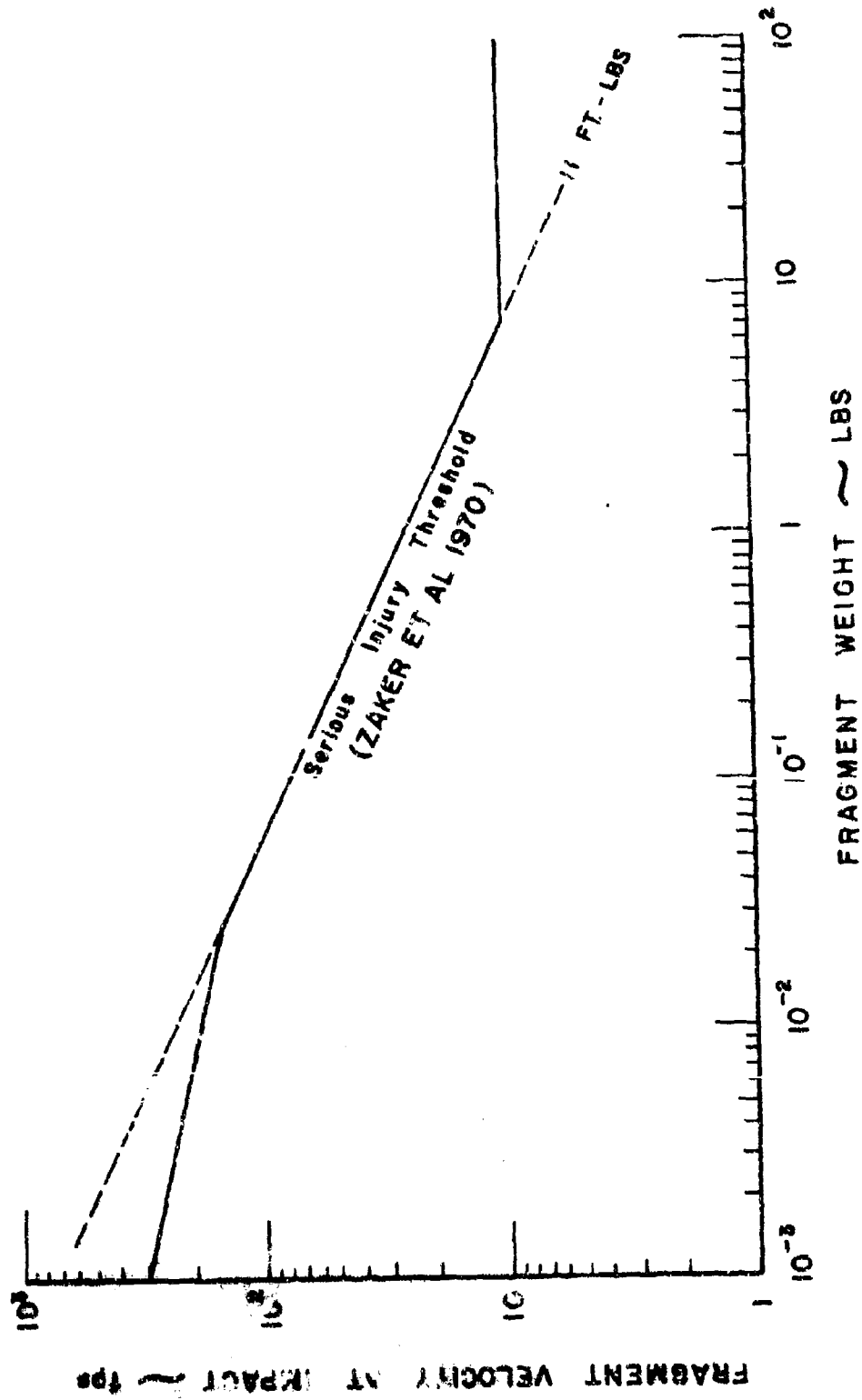


Figure 6 VULNERABILITY OF STANDING PERSONNEL TO FRAGMENTS

a nuisance type repair. Again, energy criteria normally describe those damage mechanisms. This also applies to vehicles unless the fragment strikes an important part of the engine, transmission or axle, etc.

Table 9

ENERGY LEVELS ASSOCIATED WITH PERSONNEL INJURY FROM FRAGMENTS

Injury Level	Energy, ft-lb
Threshold	11
90% Injury (10% Fatal)	40
50% Injury (50% Fatal)	58
10% Injury (90% Fatal)	85

Approximate fragment mass range where this mechanism is dominant is

$m \leq 2$ lb.

CHAPTER 9

FRAGMENT DATA

9.1 Single-Munition Fragment Density

The best data on fragment densities from single munitions at large ranges are the theoretical calculations of Feinstein and Zaker (Feinstein, 1972; Zaker et.al. 1970). In this section are presented the results of Feinstein's latest calculations of fragment densities for the four single munitions. The munitions lie on the surface with the axis parallel to the surface. The fragment density at large range is calculated for an isotropic target, i.e., a sphere of unit cross-section tangent to the surface. These densities are calculated by integrating the ballistic trajectories of the fragments using arena data for the number of fragments in each mass interval, and initial fragment velocity as a function of the azimuth angle measured from the nose. This density is related to the fragment density on the ground surface through the relation

$$Q_1(R) = \frac{Q(R)}{\sin^2 \alpha_p}$$

where:

$Q_1(R)$ is the fragment density at R for the isotropic target

$Q(R)$ is the fragment density at R at the ground surface

α_p is the angle of incidence of the fragment trajectory at impact.

Consideration of the isotropic target gives a more realistic estimate of the number of hazards that might strike a standing target, whereas the number density on the flat ground, $Q(R)$, gives an estimate for prone targets. The maximum fragment densities occur in the sidespray direction, i.e., normal to the axis of the munition. Feinstein calculated the fragment densities for all angles and the sector averages. Figures 7 through 10 show $\{Q_1(R)\}$ as a

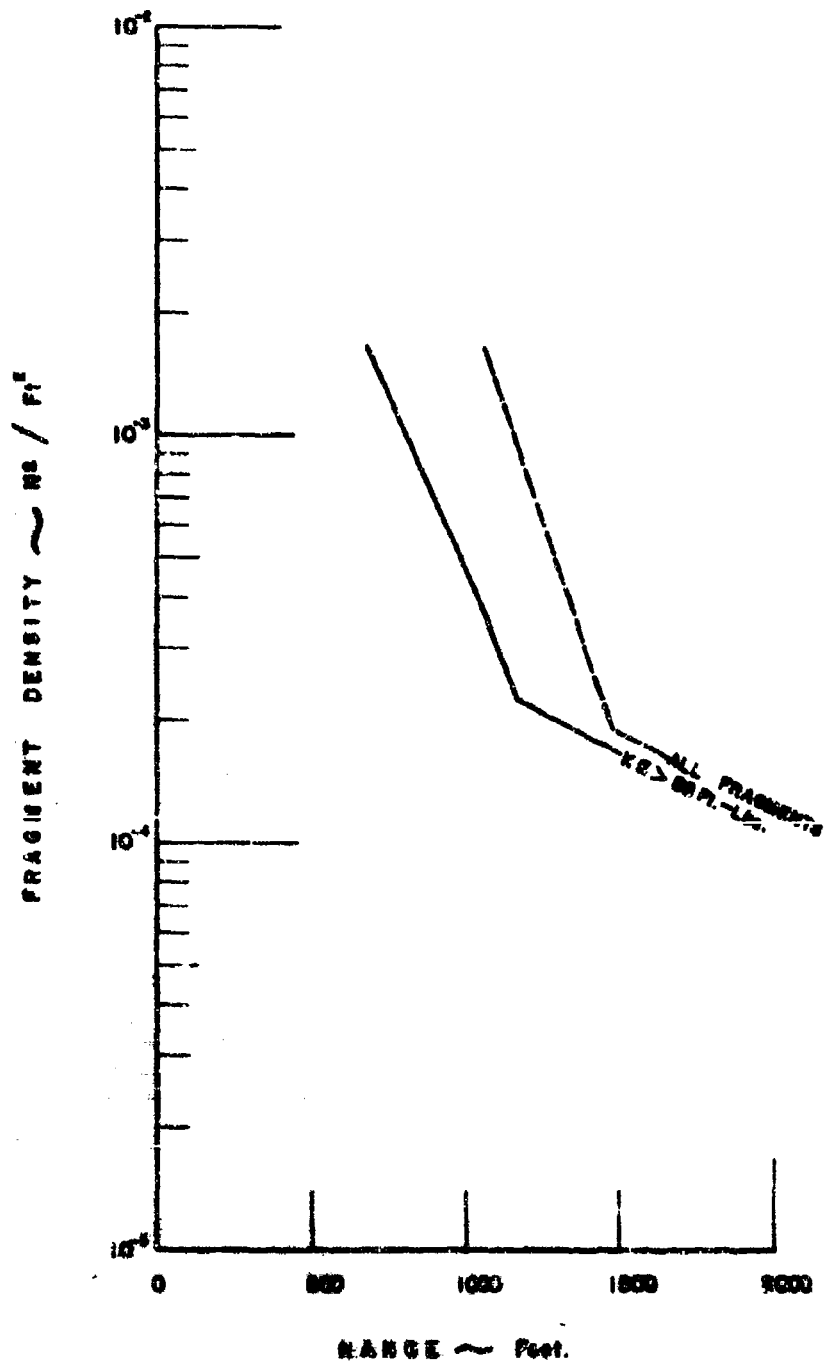


Figure 7 SINGLE MUNITION FRAGMENT DENSITY VS RANGE
 MUNITION MK 82 50-LB BOMB (FEINSTEIN 1972).

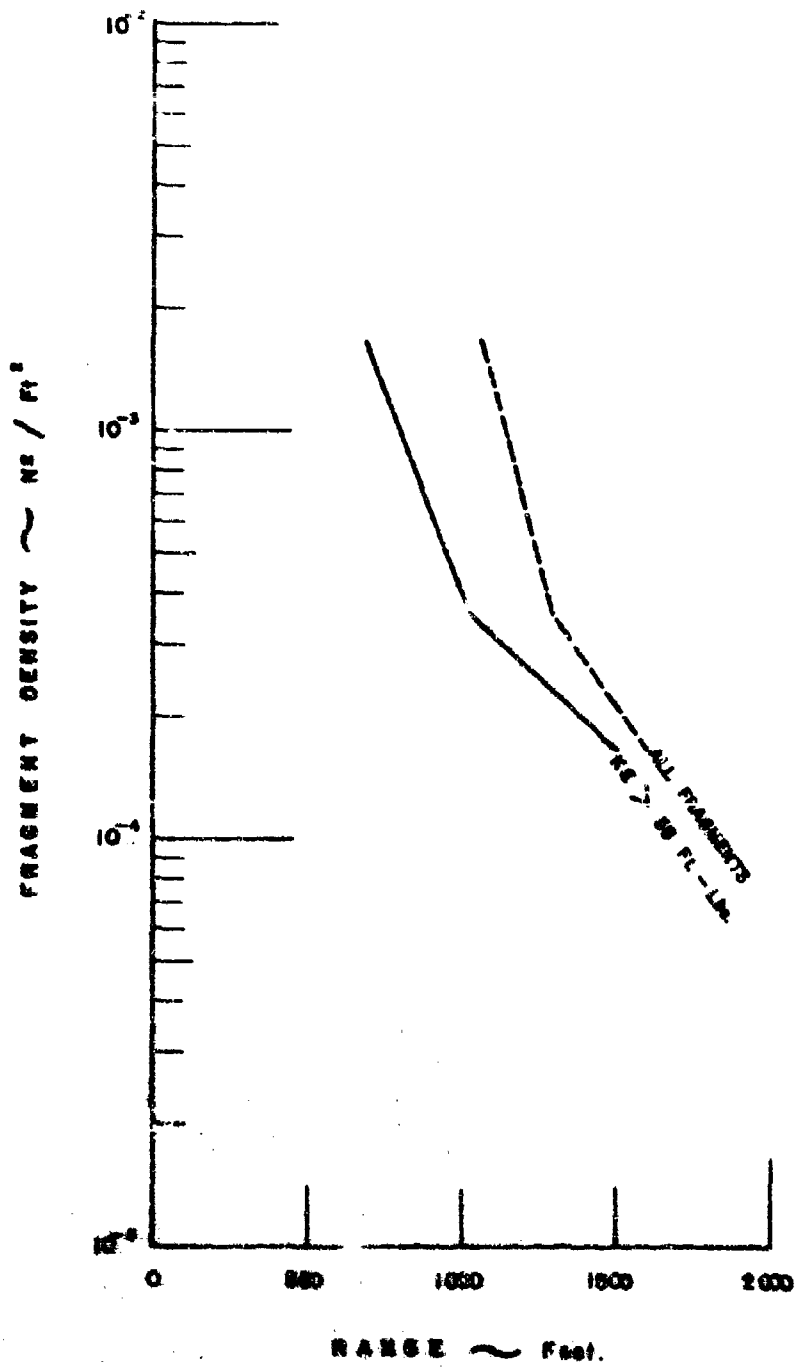


FIGURE 2 SINGLE MUNITION FRAGMENT DENSITY VS RANGE
 SHOOTING DIST TOWLE BOMB (PENNYFEIN 1972).

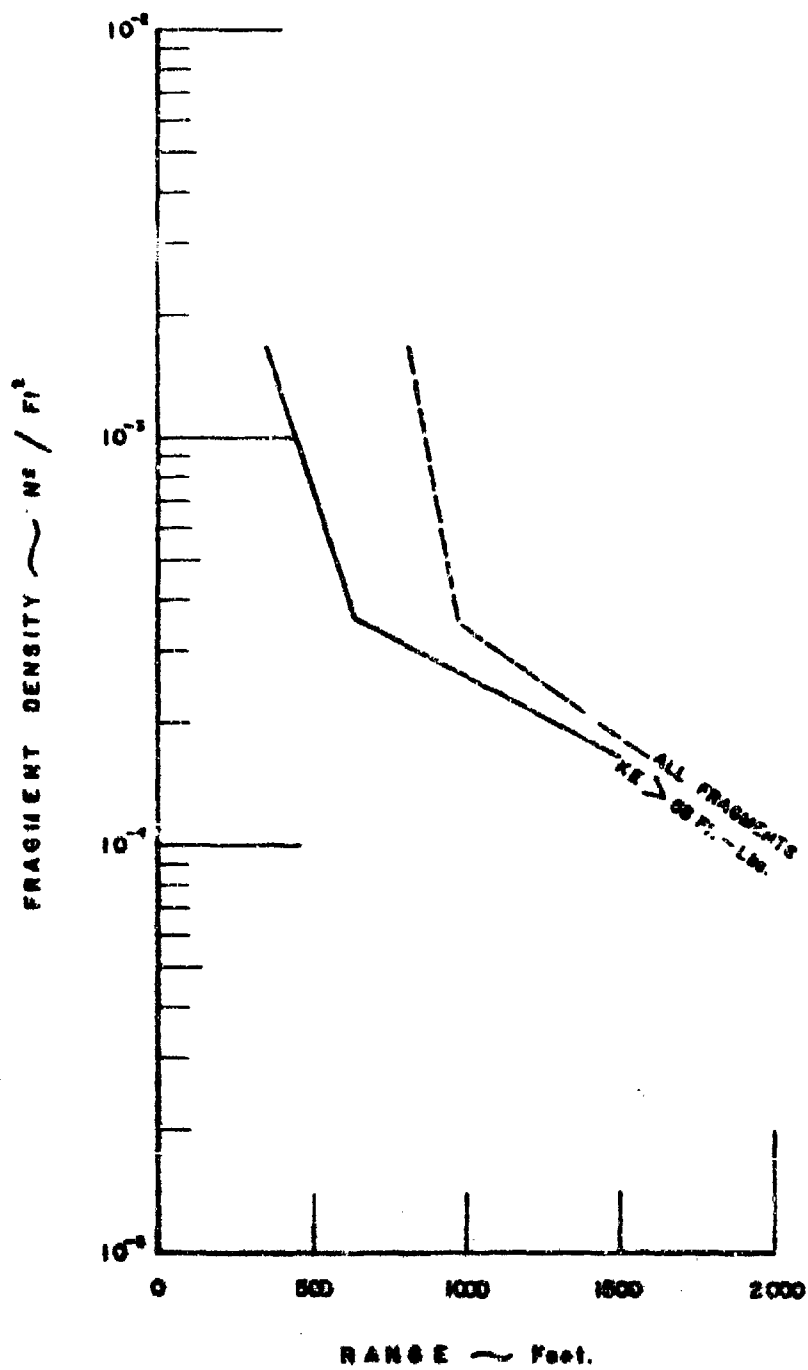


Figure 8 SINGLE MUNITION FRAGMENT DENSITY VS RANGE
 MUNITION 100mm SHELL (PENSTEIN 1972).

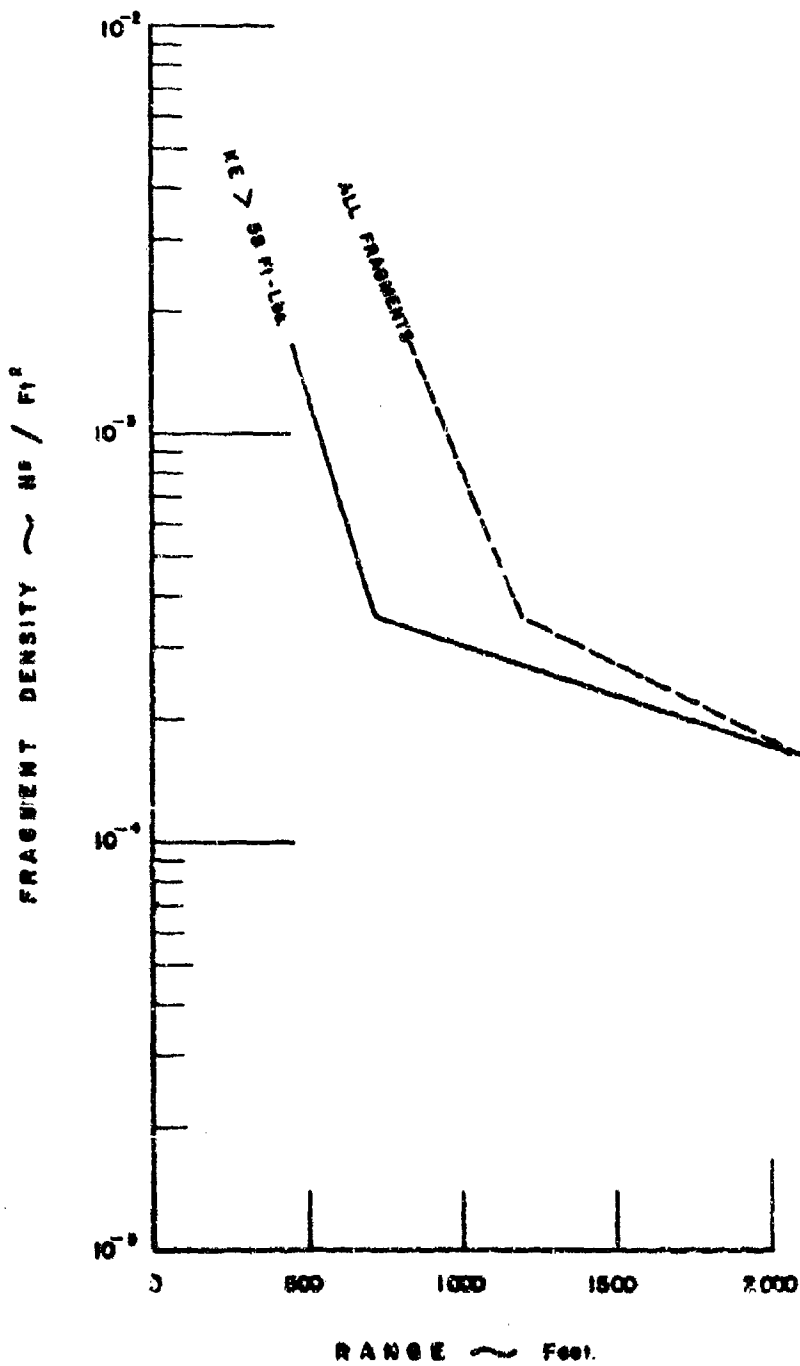


Figure 10 SINGLE MUNITION FRAGMENT DENSITY VS RANGE
MUNITION M43A2 120mm SHELL (FEINSTEIN 1972)

function of R for the four single munitions, when $\{Q_i(R)\}$ is the maximum sector average. The number densities for all fragments and for fragments with terminal kinetic energy exceeding 58 foot-pounds are shown.

The maximum sector-average fragment densities occur in the side spray direction in all cases except for the largest range for the MK82, where the greatest fragment density occurs in the nose direction. The fragment densities are shown for ranges greater than that where the number of fragments exceeds one per 600 square feet. (This is the DDESB standard range for 1-percent probability of a prone person being struck by a fragment.) Table 10 shows the range for a fragment density of 1 per 600 sq. ft. for all fragments, and for those with a kinetic energy greater than 58 foot-pounds.

Table 10

RANGES AT WHICH FRAGMENT DENSITIES (SECTOR AVERAGES)
ARE 1 PER 600 SQ. FT. (AFTER FEINSTEIN 1972)

Munition	Range, Ft.	
	All Fragments	Fragments with KE > 58 ft-lb
MK82	825	670
M117	690	1060
M107	400	810
M437A2	450	840

9.2 Stacked-Munition Fragment Density

Extension of single-munition fragment distribution to the dispersal from a stack is a difficult problem. Limited theoretical and experimental data are available. Feinstein and Nagaoka (1971) measured the dispersal from small cylinders, and demonstrated enhancement of fragment density in certain angular regions. They also measured the fragment patterns from

small stacks of 750-lb bombs. No single multiplicative factor to convert single-munition fragment data to stacked-munition fragment data is available. The assumption that only the outer layer of munitions contributes to the fragment pattern is reasonable and should give a bound to the fragment pattern.

For a row of cylinders in rectangular array with spacing $c = \pi/2$, where r is the radius of the cylinder, the number density of fragments normal to the surface and close to the array is increased to approximately

$$N_a = (0.6(n - 1) + 1)N_1$$

where:

n is the number of cylinders on the face of the array (Figure 11a)

N_1 is the number density of fragments for one cylinder

N_a is the number density for the array.

For closer spacing the coefficient 0.6 increases. N_a is approximately independent of the depth of the array.

An estimate for fragment density from a stack based on this data was made. Consider a stack n units high, m units wide on the side, and p units deep (Figure 11). The majority of fragments that are propagated to large range are ejected from the side of the stack. The fragments ejected from the top layer go essentially straight up, come straight down and remain in the vicinity of the stack. The approximation to the number density at large ranges and large stack sizes is

$$Q_2(R) = 2nm Q_1(R)$$

where:

$Q_2(R)$ is the number density for the stack in the side spray direction

$Q_1(R)$ is the fragment density for one munition in the side spray direction

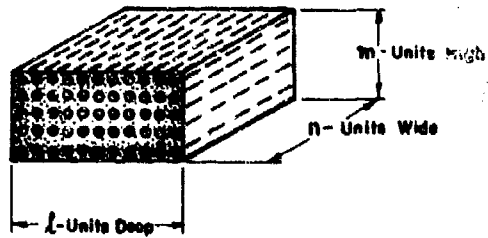


Figure 11c. STACKED MUNITION

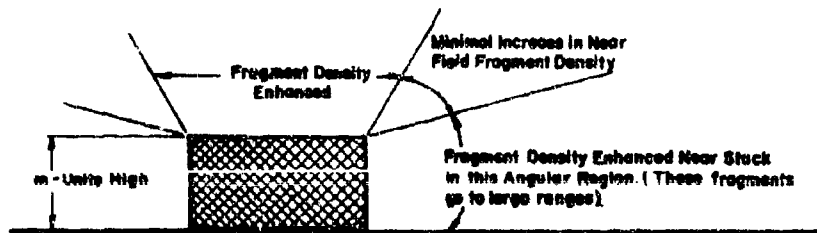


Figure 11b. SCHEMATIC FIGURE TO SHOW BASIS FOR APPROXIMATION OF FAR FIELD FRAGMENT DENSITY FROM A STACKED MUNITION.

nm is the number of munitions in the surface layer on the sides

β is a constant.

The constant β is dependent on inter-munition spacing and is slightly dependent on the number of munitions below the surface layer. From the cylinder data we expect $0.6 < \beta < 2.4$. From the small stack experiments on 750-lb bombs, the choice $\beta \approx 1$ is reasonable.

Figure 12 shows the comparison between the experimental fragment density from both a 2 x 3 x 1 and a 5 x 3 x 1 stack of M117 750-lb bombs and this model. Three units are on the side nearest the fragment measurements in both cases. Feinstein's calculation for one munition is multiplied by three. The agreement is fairly good.

This model for calculating fragment densities is quite crude and does not exhibit dependence on any stack parameters save the number of munitions on the face of the stack. This fragment density estimate should be used with extreme caution.

The calculations for single munitions show an extremely rapid fall-off of fragment density with increasing range. Since there is a maximum fragment size, there is a maximum range beyond which no fragments will be found. Using a simple multiplicative factor to determine the fragment density from a stack again indicates rapid fall-off with range, and the same limiting range beyond which there are no fragments.

9.3 Damage Probability

The probability of being injured by a fragment from a single munition is (Zaker et al., 1970)

$$P_1(R) = 1 - \exp(-Q_1(R)A)$$

where A is the presented area of the target. For personnel standing in the open in the far-field the presented area is the maximum horizontal cross-

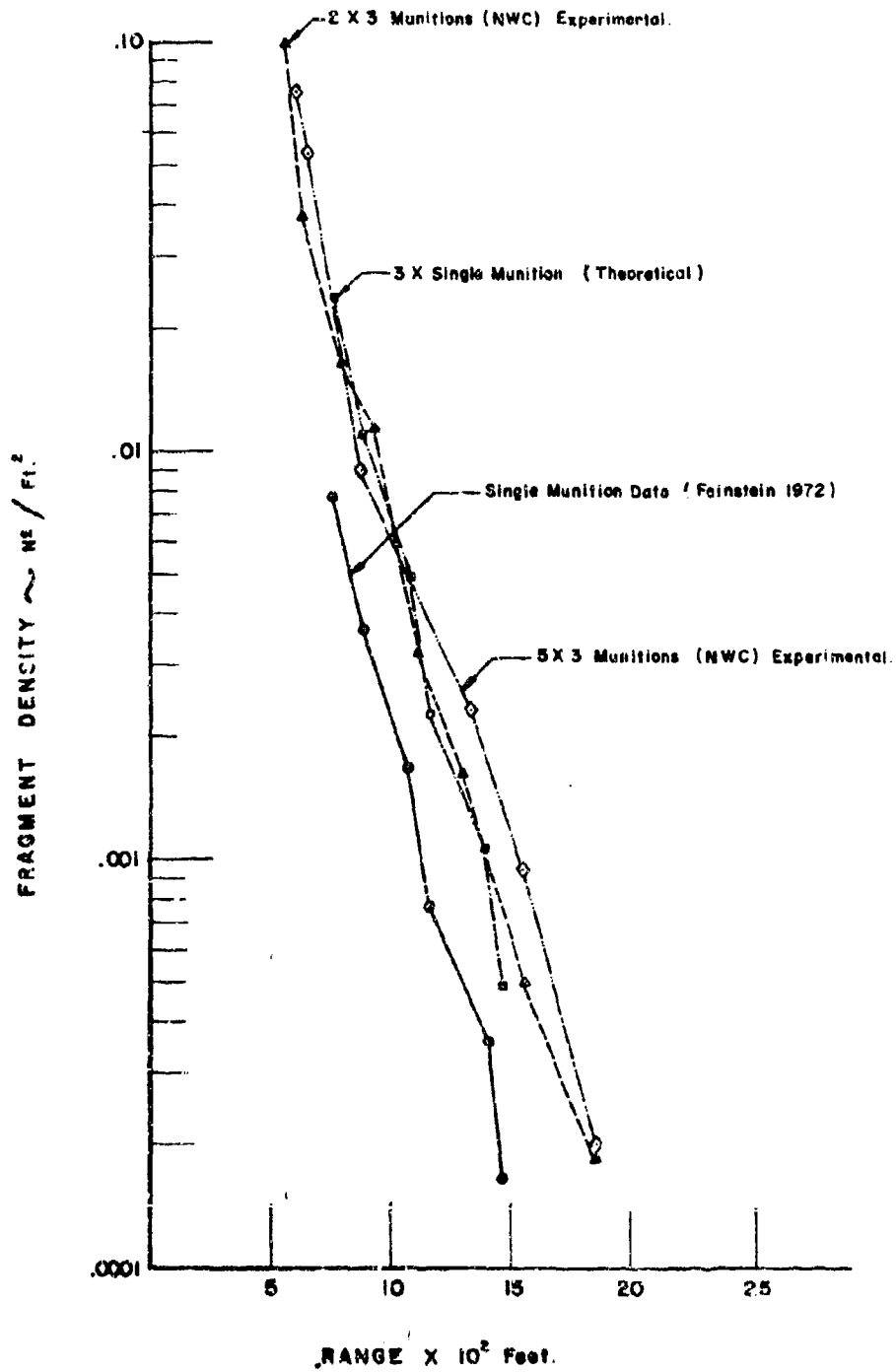


Figure 12 CALCULATED FRAGMENT DENSITY FOR STACKED MUNITIONS FROM THE SINGLE MUNITION MODEL.

section area of the body and is approximately $4/3$ square feet. If $Q(R)$ is small i.e., $Q(R) \ll 1$,

$$P_1(R) \approx \frac{4}{3} Q_1(R)$$

Applying a simple multiplicative formula for the fragment density from a stack

$$Q_n(R) = n Q_1(R)$$

Thus,

$$\begin{aligned} P_n(R) &= 1 - (1 - P_1(R))^n \\ &\approx \frac{4}{3} n Q_1(R) \quad nQ_1(R)A \ll 1 \end{aligned}$$

The presented area for critical damage to a vehicle is quite small. Consider, for example, a readily breakable part of the engine, typically a distributor, which has a presented area of approximately 0.2 square foot.

CHAPTER 10

CRITIQUE OF FRAGMENT HAZARD EVALUATION

The fragment density profiles presented in Chapter 10 are theoretical predictions based on single-munition arena data. Experimental verification of the fragment densities expected from stacked munitions is very limited. There are little experimental and no theoretical data on the effect of fragment hazards for munitions within a magazine or igloo. A certain percentage of fragments are stopped or retarded by the cover, and in addition, fragments are generated by the breakup of the cover as a result of the detonation. Since no data were available on this screening and fragment generation, no attempt was made to present fragment densities for confined storage configurations.

The interaction of fragments from adjacent munitions in a stack is also not well determined, either theoretically or experimentally, although some limited data allowed for a crude estimation of stacked-munition fragment densities using single-munition fragment data.

It is our recommendation that these two problems be investigated on a theoretical and experimental basis. The theoretical studies should be undertaken to determine the parametric relationship of far-field fragment densities to single-munition fragment predictions, and the stack and confinement parameters.

It is further suggested that DDESB conduct experiments designed to correlate the single-munition far-field fragments from munitions stacked in the open, behind barricades and within igloos. The total experimental plan might contain the following elements:

1. Far-field fragment data from a single munition, both horizontal and vertical, in the open, behind a revetment and within an igloo.
2. Far-field fragment data from several selected stacks in the open.
3. Far-field fragment data from several selected stacks behind earth revetments.
4. Far-field fragment data from several selected stacks within an igloo.

The sizes of the stacks need not be large, but must be designed to obtain information on the stack, and the effects of its parameters on the fragment data. If the number and types of stacks in Part 2 are judiciously chosen, fewer experiments in Parts 3 and 4 will be needed to determine the effects of the barricades and covers. It is important that a single munition be used throughout so that correlations between various configurations can be established.

REFERENCES

- Adams, C. L., Sarmousakis, J.N. and Sperrazza, J. (1949) "Comparison of the Blast from Explosive Charges of Different Shapes", BRL Report 681.
- Army Navy Explosives Board (1947) "Igloo Tests", Technical Paper No. 3.
- Army Navy Explosives Safety Board (1946a) "Scale Model Igloo Magazine Explosives Tests", Technical Paper No. 4.
- Army Navy Explosives Safety Board (1946b) "Igloo and Revetment Tests", Technical Paper No. 5.
- Bowen, I. G. et al., (1968) "Estimate of Man's Tolerance to the Direct Effects of Air Blast," DASA 2113.
- Coder, J. D. (1971) "Opening Remarks for Review of Current Explosives Safety Standard Evaluations Eskimo I - Igloo Test", Thirteenth Explosives Safety Seminar, 29-30.
- Custard, G. H. et al., (1970), "Evaluation of Explosive Storage Safety Criteria", Final Report, Contract DAHC04-69-C-0095.
- Ethridge, N. (1961) "Vehicle Response Study" in United States Participation in 1961 Canadian 100-Ton High-Explosive Test (U) - Preliminary Report DASA-1249, 114-143 (C).
- Feinstein, D. I., (1971) "Fragment Hazard Criteria", Thirteenth Explosives Safety Seminar, 429-436.
- Feinstein, D. I., (1972) "Fragmentation Hazards to Unprotected Personnel", Final Report, Contract DAHC-04-69-C-0052.
- Feinstein, D. I., and Nagacka, K. H., (1971) "Fragmentation Hazard Study - Fragment Hazards from Detonation of Multiple Munitions in Open Stores", Final Report Contract DAHC-04-69-C-0056.
- Fugelso, L. E., Fields, S. F. and Byrne, W. J. (1971) "Dial Pack Blast Directing Experiment, 42nd Shock and Vibration Symposium.
- Glasstone, S., (1964) Effects of Nuclear Weapons, 2nd Ed.
- Hirsch, F. G. (1966) "Effects of Overpressure on the Ear - A Review", DASA 1858.
- Johnson, O. T. (1967) "A Blast Damage Relationship", BRL Report 1389.
- Joint Munitions Effectiveness Manual (1970) (C).
- Kennedy, W. D. (1946) "Explosions and Explosives in Air", in Effects of Impact and Explosion, OSRD, Division 2, Summary Technical Report.
- Kingery, C. H. (1966) "Air Blast Parameters Versus Distance for Hemispherical TNT Surface Bursts", BRL R1344.

REFERENCES
(CONT'D)

- Kingery, C. N. (1970) "Air Blast From 155mm Stack Separation Tests", 12th ASESB Seminar, 411-416.
- Peterson, F. H. et al. (1968) "High Explosive Storage Tests - Big Papa", AFWL TR-67-132.
- Richmond, D. R. et al. (1966) "Biological Effects of Blast and Shock", DASA 1777.
- Richmond, D. R. et al. (1968) "The Relationship between Selected Blast Wave Parameters and the Reponse of Mammals Exposed to Air Blast", Ann. N.Y. Acad. Sci., 152, 103-121.
- Richmond, D. R. and Fletcher, E. R. (1971), "Blast Criteria for Personnel in Relation to Quantity Distance", 13th ASESB Seminar, 401-419.
- Von Gierke, H. (1968) "Response of the Body to Mechanical Forces", Ann. N.Y. Acad. Sci., 152, 172-186.
- Westine, P. S. (1971) "R-W Plane Analysis for Vulnerability of Targets to Air Blast", 42nd Shock and Vibration Symposium.
- Wiedermann, A. H. (1970) "Blast Wave Diffraction over Barricades", 12th ASESB Seminar, 245-265.
- Wilton, C. (1970) "Building Damage Surveys from Explosion Tests", 12th ASESB Seminar, 267-286.
- Witsotski, J. and Snyder, W. H. (1965) "Characteristics of Blast Wave Obtained from Cylindrical High Explosive Charges" DRI-2286.
- Zaker, T. A. et al. (1970) "Fragmentation Hazard Study, Phases I and II," Final Report, Contract DAHC-04-69-C-0056.